物 理 化 学 学 报
Acta Phys. -Chim. Sin. **2018,** *34* (X), 0001–0009 0001

[Article] doi: 10.3866/PKU.WHXB201712151 www.whxb.pku.edu.cn

Electronic Stability of Eight-electron Tetrahedral Pd_4 Clusters

SHEN Yanfang [1], CHENG Longjiu [1,2,*]

[1] School of Chemistry and Chemical Engineering, Anhui University, Hefei 230601, P. R. China.

[2] Anhui Province Key Laboratory of Chemistry for Inorganic/Organic Hybrid Functionalized Materials, Hefei 230601, P. R. China.

Abstract: Motivated by the unusual structure of the $[Pd_4(\mu_3\text{-}SbMe_3)_4(SbMe_3)_4]$ cluster, which is composed of a tetrahedral (T_d) Pd(0) core with four terminal $SbMe_3$ ligands and four triply bridging $SbMe_3$ ligands capping the four triangular Pd_3 faces (*J. Am. Chem. Soc.* **2016,** *138*, 6964), we performed a computational study of the structure and bonding characteristics of the T_d $[Pd_4(\mu_3\text{-}SbH_3)_4(SbH_3)_4]$ cluster and a series of its analogues. The T_d structure of the $[Pd_4(\mu_3\text{-}SbH_3)_4(SbH_3)_4]$ cluster could be explained by the cluster electron-counting rules based on the 18-electron rule for transition-metal centers; each sp^3 hybridized Pd atom contributed ten valence electrons, and eight valence electrons were provided by one terminal SbH_3 and three bridging μ_3-SbH_3 ligands. The $[Pd_4(\mu_3\text{-}SbH_3)_4(SbH_3)_4]$ cluster had a count of 104 valence electrons in total; chemical bonding analysis indicated that the cluster featured twenty electron lone pairs generated by *d* orbital of the four Pd atoms, twenty-four Sb—H σ bonds, four terminal Pd—Sb σ bonds, and four delocalized bonds. There were two bonding patterns of the eight delocalized electrons between the four capping Sb atoms and the Pd_4 core. The first pattern was based on the superatom-network (SAN) model, whereby the palladium cluster could be described as a network of four $2e^-$ superatoms. The second pattern was based on the spherical jellium model, whereby the cluster could be rationalized as an $8e^-$ $[Pd_4(\mu_3\text{-}SbH_3)_4]$ superatom with $1S^21P^6$ electronic configuration. The density functional theory (DFT) calculations showed that the T_d $[Pd_4(\mu_3\text{-}SbH_3)_4(SbH_3)_4]$ cluster had a large HOMO-LUMO (HOMO: highest occupied molecular orbital; LUMO: lowest unoccupied molecular orbital) energy gap (2.84 eV) and a negative nucleus-independent chemical shift (NICS) value (−12) at the center of the $[Pd_4(\mu_3\text{-}SbH_3)_4(SbH_3)_4]$ cluster, indicating its high chemical stability and aromaticity. Furthermore, the NICS values in the range of 0–0.30 nm of the $[Pd_4(\mu_3\text{-}SbH_3)_4]$ motifs were much more negative than those of $[Pd_4(SbH_3)_4]$ in the same range, revealing that the overall stability of $[Pd_4(\mu_3\text{-}SbH_3)_4(SbH_3)_4]$ was likely derived from the local stability of $Pd_4(\mu_3\text{-}SbH_3)_4$. Meanwhile, the $d^{10}\cdots d^{10}$ interaction played a critical role in stabilizing the Pd_4 tetrahedron structure, which is similar to the aurophilicity in Au-Au clusters. It was also found that there is a large difference in the stability of transition metal and non-transition metal clusters with a tetrahedron structure. The structures and bonding patterns of the designed analogues were similar to those of $[Pd_4(\mu_3\text{-}SbH_3)_4(SbH_3)_4]$. To summarize, this study was relevant for deciphering the nature of the bonds in a tetrahedral complex with four cores and eight ligands, and predicting a series of analogues. It is expected that this work will provide more options for the synthesis of tetrahedral 4-core transition metal compounds.

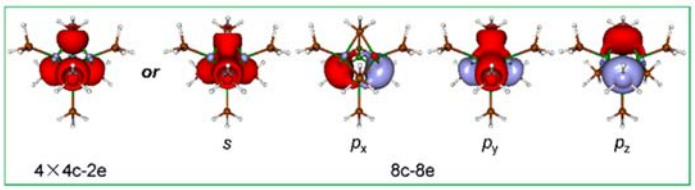

Key Words: Metal cluster; Super valence bond; Superatom; Chemical bonding analysis; Closed-shell interaction; Aromaticity

Received: October 31, 2017; Revised: November 29, 2017; Accepted: December 11, 2017; Published online: December 15, 2017.

*Corresponding author. Email: clj@ustc.edu.

The project was supported by the National Natural Science Foundation of China (21573001), and the Foundation of Distinguished Young Scientists of Anhui Province, China.

国家自然科学基金(21573001)和安徽省杰出青年科学家基金资助项目

八电子 Pd_4 四面体团簇的电子结构稳定性分析

沈艳芳[1]，程龙玖[1,2,*]

[1] 安徽大学化学化工学院，合肥 230601

[2] 安徽省有机/无机杂化功能材料重点化学实验室，合肥 230601

摘要：基于理论计算，我们报道了T_d对称性的[$Pd_4(\mu_3\text{-}SbH_3)_4(SbH_3)_4$]团簇及一系列类似物的结构与成键。成键分析表明：每个Pd原子都是sp^3杂化，其10个价电子与四个配体提供的8个价电子，满足18电子规则。并且，每个Pd原子与四个桥连的SbH_3配体可以形成四个离域的四中心两电子超级σ键或八中心两电子键。一方面，根据超原子网络模型，这个钯团簇可以描述成四个2电子的超原子网络。另一方面，凝胶模型表明，它可以合理化的作为电子组态是$1S^21P^6$的8电子超原子。与此同时，$d^{10}\cdots d^{10}$闭壳层相互作用在稳定Pd_4四面体结构中起到了关键性的作用。密度泛函理论计算表明：T_d对称性[$Pd_4(\mu_3\text{-}SbH_3)_4(SbH_3)_4$]团簇表现出高度稳定性，具有充满的电子壳层，大的HOMO-LUMO带隙(2.84 eV)以及负的核独立化学位移(NICS)值。此外，基于[$Pd_4(\mu_3\text{-}SbH_3)_4(SbH_3)_4$]结构与成键模式，我们设计了一系列稳定的类似物，其有可能被实验合成出来。

关键词：金属团簇；超价键；超原子；化学键分析；闭壳层相互作用；芳香性

中图分类号：O641

1 Introduction

Clusters composed of atoms display unique physical, chemical and electronic characteristics that have attracted considerable attention in recent years, of which metal clusters is one of the most essential parts [1–15]. The first major breakthrough was the observation on “magic numbers” in the mass spectra of free sodium made by Knight and co-workers in 1984 [16], to the extent that much effort was put to understanding their stability in the factor of electronic shell. The first reasonable explanation was on the basis of the spherical jellium model proposed by Clemenger and co-workers [17]. In this model, the electronic levels of metal clusters are $1S^2|1P^6|1D^{10}|2S^21F^{14}|2P^61G^{18}|\cdots$, which is associated with the magic numbers 2, 8, 18, 20, 34, 40, 58, ⋯. Moreover, the fact along with similarity in stability and chemical nature between simple metal clusters and individual atom, the superatom electronic theory has been successful explaining the mass abundances of gas-phase metallic clusters [18]. Khanna, Jena and Castleman presented that the magic-number metal clusters could be viewed as superatoms [19–23].

However, there is no a reasonable explanation to the nonspherical clusters and sub-peaks in the mass spectra by spherical jellium model. In 2013, our group proposed a super valence bond (SVB) model [24], of which the shell closures of superatoms were obtained by sharing valence pairs and nuclei with superatoms or ligands. This model has been ideally applied in Li clusters (Li_{26}, Li_{14}, Li_{10}, Li_8), Au clusters (Au_{23}^{+9}, Au_{20}^{+6}, Au_{20}) and other metal clusters [24–31].

The chemistry of palladium is one of the most extensive and versatile fields of chemistry, because this metal can easily form complexes with many organic and inorganic molecules [32–38]. In 2016, Benjamin and co-workers [39] synthesized an unusual [$Pd_4(\mu_3\text{-}SbMe_3)_4(SbMe_3)_4$] cluster which is composed of a tetrahedral Pd(0) core with four terminal $SbMe_3$ ligands and four triple bridging $SbMe_3$ ligands capping four triangular Pd_3 faces, inevitably attracting our attention. Theoretical research shows that both bridging and terminal $SbMe_3$ ligands can help to stabilize the electron rich Pd_4 core as efficient acceptors in metal-to-ligand π-back-donation. What motivated us to investigate this complex is the unusual geometric shape and complicated electronic structure. We want to see whether the above models can be used to illustrate the stability of this Pd cluster. Our aim is, therefore, to decipher bond nature of the 4-core 8-ligands tetrahedral complex and predict a series of analogues. The understanding of bonding nature between the two kind of ligands and 4-core metal clusters should provide more possibilities to the synthesis of transition metal compounds.

2 Computational methods

The geometries of the studied system in this work are fully optimized at TPSSh/def2-TZVP level. The vibrational frequencies are computed to check whether the obtained structure is a true minimum point with all real frequencies. We also apply the same level to calculate the HOMO-LUMO gaps (E_{HL}), NICS and binding energies. NICS value is a popular measurement for aromaticity, where negative value shows aromaticity, and positive value suggests antiaromaticity. Adaptive natural density partitioning (AdNDP) developed by Boldyrev’s group [40] is carried out using PBE method with the basis set of LANL2DZ, in order to elucidate the chemical bonding of these clusters. All calculations are done with Gaussian 09 package [41]. The visualization of the AdNDP results is realized using the MOLEKEL 5.4.0.8 program [42].

3 Results and discussion

3.1 Geometry structure

The initial coordinates of $[Pd_4(\mu_3\text{-}SbMe_3)_4(SbMe_3)_4]$ are obtained from crystal data of the Benjamin paper [39]. For the convenience of going into the electronic structure of cluster, all methyl groups are replaced with H atoms and optimized at TPSSH/def2-TZVP level (Fig. 1). The ultimate cluster structure is T_d $[Pd_4(\mu_3\text{-}SbH_3)_4(SbH_3)_4]$. The optimized Pd-Pd distance of Pd_4 unit and bond length of Pd-$Sb_{S/V}$ (μ_3-Sb)/terminal Sb atoms) are 0.2792 nm and 0.2790/0.2537 nm, respectively. Theoretical results are in good agreement with the corresponding experimental values (0.2805 nm and 0.2773/0.2520 nm, respectively). The $[Pd_4(\mu_3\text{-}SbH_3)_4(SbH_3)_4]$ cluster has an tetrahedron Pd_4 metal core stabilized by eight ligands. It can be seen that all Pd_3 faces of tetrahedron are fully capped by SbH_3 ligands and all Pd atoms are coordinated to terminal SbH_3 ligands.

3.2 Electronic structure

Why is this tetrahedron cluster stable? First, we concentrate on the nature of the bonding in this structure by using AdNDP method which is wildly applied for closed-shell species recovering both the classical Lewis bonding concepts (lone-pairs and two-center two electron (2c-2e) bonds) and the delocalized *n*-center two electron (*n*c-2e) bonds [43–53].

The T_d $[Pd_4(\mu_3\text{-}SbH_3)_4(SbH_3)_4]$ possesses 104 valence electrons in total. AdNDP analysis (Fig. 2) identifies twenty

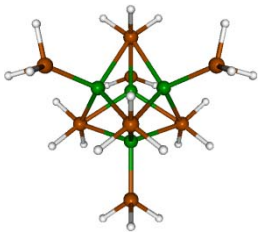

Fig. 1 Optimized T_d structure of $[Pd_4(\mu_3\text{-}SbH_3)_4(SbH_3)_4]$ cluster at the TPSSh/def2-TZVP level.

Pd-green; Sb-brown; H-white.

lone pairs with occupy numbers (ONs) lying within the range of 1.90–2.00 |e|, which are generated by the *d* orbital electrons of four Pd atoms. There exist clearly 24 Sb—H σ bonds, which consume 48 electrons. This remains 16 electrons, with each Sb atom contributing two valence electrons. 8 electrons are localized along the four terminal Sb—Pd dative bonds. The other 8 electrons are delocalized between four capping Sb atoms and Pd_4 core. AdNDP analysis gives two bonding patters of the 8 electrons of $[Pd_4(\mu_3\text{-}SbH_3)_4(SbH_3)_4]$. Pattern I is based on the SAN model proposed by Cheng *et al*. [24], this 8e cluster should be taken as a network of four 4c-2e tetrahedral $PdSb_3$ superatoms. As expected, AdNDP reveals four 4c-2e delocalized super σ-bonds with ON = 1.96 |e| in each $PdSb_3$ units, which suggests that $[Pd_4(\mu_3\text{-}SbH_3)_4]$ includes four $PdSb_3$ close-shell 2e superatoms, making the $[Pd_4(\mu_3\text{-}SbH_3)_4]$ as an

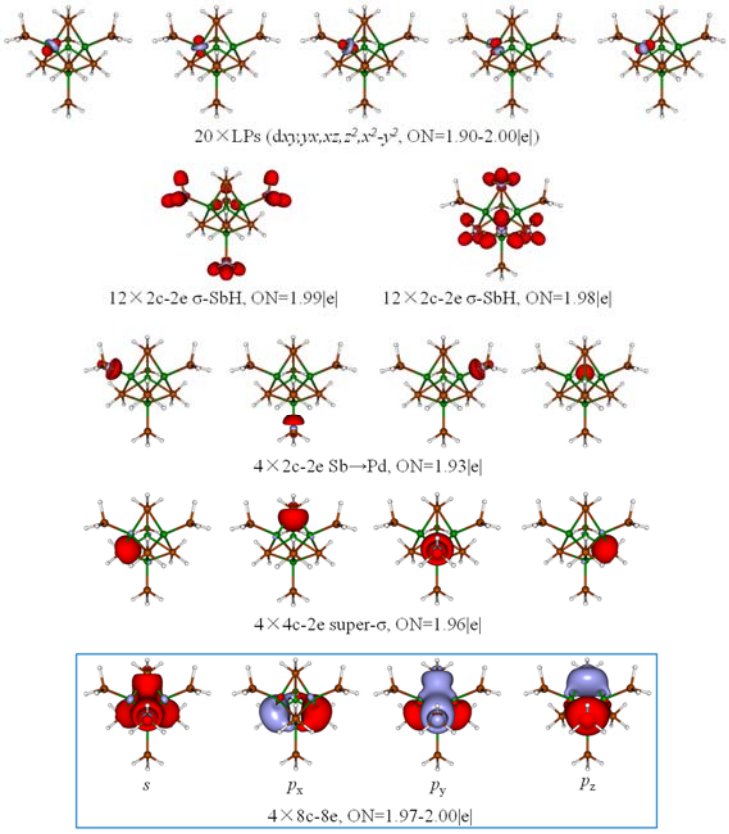

Fig. 2 Bonding pattern for T_d $[Pd_4(\mu_3\text{-}SbH_3)_4(SbH_3)_4]$ cluster as revealed from the AdNDP analysis.

Occupation numbers (ONs) are shown.

eight electron shell. Pattern II is according to the spherical jellium model, this electron number is consistent with the superatom concept and corresponds to the closed-shell $1S^2 1P^6$ configuration. [$Pd_4(\mu_3\text{-}SbH_3)_4$] is found with one super *S* (ON = 2.00 |e|) and three *P* ($P_{x,y,z}$) (ON = 1.97 |e|) 8c-2e orbitals.

With the geometric shape and electronic structure of [$Pd_4(\mu_3\text{-}SbH_3)_4(SbH_3)_4$], each Pd atom is in $4d^{10}$ configuration and coordinated to one terminal Sb atom and three bridging Sb atoms, of which sp^3 empty orbitals are occupied with 8 electrons contributed by four Sb atoms, rendering 18-electrons principle. Meanwhile, [$Pd_4(\mu_3\text{-}SbH_3)_4$] obtains closed shells by sharing electronic pairs with ligands, being of 8e superatom.

Since the delocalization is an important cause of aromaticity, and aromaticity is usually associated with the high stability, we carry on the study on the aromaticity for this cluster. We believe the aromaticity of $Pd_4(\mu_3\text{-}SbH_3)_4$ is also a key part to govern the stability of T_d [$Pd_4(\mu_3\text{-}SbH_3)_4(SbH_3)_4$]. Herein, NICS-scan method is employed to analyze the aromaticity of this cluster. The aromatic properties along *z*-axes (coined as NICSzz-scan) within the range of 0–0.30 nm from center to out-of-plane of $Pd_4(\mu_3\text{-}SbH_3)_4$, $Pd_4(SbH_3)_4$ and $Pd_4(\mu_3\text{-}SbH_3)_4(SbH_3)_4$ are calculated. Fig. 3 plots the NICSzz-scan curves for $Pd_4(\mu_3\text{-}SbH_3)_4$, $Pd_4(SbH_3)_4$ and $Pd_4(\mu_3\text{-}SbH_3)_4(SbH_3)_4$. In the case of $Pd_4(SbH_3)_4$ motifs, the NICS values are almost positive, meaning its antiaromaticity. However, all negative NICS values suggest aromaticity of $Pd_4(\mu_3\text{-}SbH_3)_4$, in contrast to the antiaromaticity of $Pd_4(SbH_3)_4$. For T_d [$Pd_4(\mu_3\text{-}SbH_3)_4(SbH_3)_4$] cluster, it also exhibits negative NICS values which are smaller than the that of $Pd_4(\mu_3\text{-}SbH_3)_4$ (within the range of 0 to 0.25 nm). What the consequence can be caused by the antiaromaticity of $Pd_4(SbH_3)_4$ and the aromaticity of $Pd_4(\mu_3\text{-}SbH_3)_4$ together. NICS calculations agree well with the AdNDP analysis. Moreover, the H-L gap of [$Pd_4(\mu_3\text{-}SbH_3)_4(SbH_3)_4$] (2.84 eV) is also very large, indicating the close-shell electronic structure of [$Pd_4(\mu_3\text{-}SbH_3)_4(SbH_3)_4$]. As predicted, we can draw a conclusion that [$Pd_4(\mu_3\text{-}SbH_3)_4(SbH_3)_4$] is stable with high aromaticity, which is based chiefly on $Pd_4(\mu_3\text{-}SbH_3)_4$.

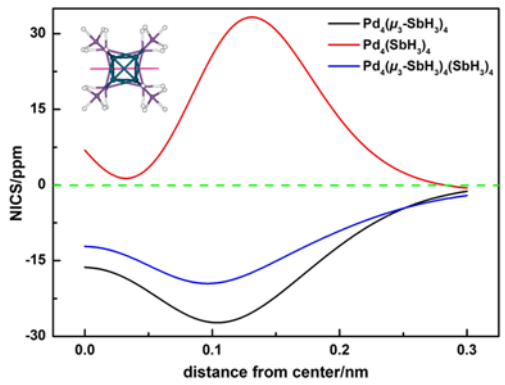

Fig. 3 The NICSzz-scan curves for $Pd_4(\mu_3\text{-}SbH_3)_4$, $Pd_4(SbH_3)_4$ and $Pd_4(\mu_3\text{-}SbH_3)_4(SbH_3)_4$ within the range of 0 to 0.30 nm from center to out-of-plane.

3.3 $M_4(\mu_3\text{-}LAH_3)_4(LBH_3)_4$

The intriguing bonding and aromatocity of $Pd_4(\mu_3\text{-}SbH_3)_4(SbH_3)_4$ have motivated us to design additional clusters. Here we certify that the new metal clusters can be also 8e superatoms by changing metal and ligand while without changing their valence electron count. Considering the Pd $4d^{10}$ and Sb $5s^2 5p^3$ configurations, we replace Pd with M (M = $4d^{10}5s^1$ Ag, $4d^{10}5s^2$ Cd, $5s^2$ Ba and $5s^2 5p^1$ In), accordingly, LA and LB (Si, Ge, Sn, Pb and Al) can be substituted for Sb.

To determine the stabilities of the series of analogues, the E_{HL} gaps are calculated and the results are listed in Table 1. By contrast, for M = Ag and Cd, these clusters possess slightly larger E_{HL} values from 2.90 to 3.68 eV as a comparison with that of $Pd_4(\mu_3\text{-}SbH_3)_4(SbH_3)_4$ of 2.84 eV. Whereas the E_{HL} values of In species are significantly smaller, the reason is probably that, the In is the main group element.

In Table 1, we also calculate the binding energies, which are defined as $E_{b\text{-}S} = E[M_4(\mu_3\text{-}LAH_3)_3(LBH_3)_4] + E[\mu_3\text{-}LAH_3] - E[M_4(\mu_3\text{-}LAH_3)_4(LBH_3)_4]$, $E_{b\text{-}V} = E[M_4(\mu_3\text{-}LAH_3)_4(LBH_3)_3] + E[LBH_3] - E[M_4(\mu_3\text{-}LAH_3)_4(LBH_3)_3]$, where $E[M_4(\mu_3\text{-}LAH_3)_3(LBH_3)_4]$, $E[\mu_3\text{-}LAH_3]$, $E[M_4(\mu_3\text{-}LAH_3)_4(LBH_3)_4]$, $E[M_4(\mu_3\text{-}LAH_3)_4(LBH_3)_3]$ and $E[LBH_3]$ represent the energies of molecules $M_4(\mu_3\text{-}LAH_3)_3(LBH_3)_4$, $\mu_3\text{-}LAH_3$, $M_4(\mu_3\text{-}LAH_3)_4(LBH_3)_4$, $M_4(\mu_3\text{-}LAH_3)_4(LBH_3)_3$ and LBH_3, respectively. For all investigated clusters, the positive $E_{b\text{-}S}$ and $E_{b\text{-}V}$ show that M_4 can bind stably with bridging and terminal ligands. In comparison, [$Pd_4(\mu_3\text{-}SbH_3)_4(SbH_3)_4$] is most stable with biggest $E_{b\text{-}S}$ and $E_{b\text{-}V}$ among these clusters. We can know that each Ag atom provides one electron to bond with Sb atom, thus, there is

Table 1 HOMO-LUMO gaps E_{HL} of $M_4(\mu_3\text{-}LAH_3)_4(LBH_3)_4$, binding energies $E_{b\text{-}S}$, $E_{b\text{-}V}$ of $M_4(\mu_3\text{-}LAH_3)_4$ and $M_4(LBH_3)_4$, respectively.

Type	Compound	E_{HL}/eV	$E_{b\text{-}S}$/eV	$E_{b\text{-}V}$/eV
0–0	$Pd_4(\mu_3\text{-}SbH_3)_4(SbH_3)_4$	2.84	6.24	6.15
0–1 [a]	$Ag_4(\mu_3\text{-}SbH_3)_4(PbH_3)_4$	2.95	5.81	2.36
	$Ag_4(\mu_3\text{-}SbH_3)_4(SnH_3)_4$	2.90	5.80	2.51
	$Ag_4(\mu_3\text{-}SbH_3)_4(GeH_3)_4$	3.05	5.81	2.65
	$Ag_4(\mu_3\text{-}SbH_3)_4(SiH_3)_4$	3.04	5.81	2.66
1–1	$Cd_4(\mu_3\text{-}PbH_3)_4(PbH_3)_4$	3.54	1.75	2.03
	$Cd_4(\mu_3\text{-}SnH_3)_4(SnH_3)_4$	3.55	1.94	2.23
	$Cd_4(\mu_3\text{-}PbH_3)_4(SnH_3)_4$	3.63	1.78	1.79
	$Cd_4(\mu_3\text{-}PbH_3)_4(SiH_3)_4$	3.68	1.80	2.36
	$Cd_4(\mu_3\text{-}SiH_3)_4(PbH_3)_4$	3.22	2.00	2.09
1–2	[b] $Ba_4(\mu_3\text{-}PbH_3)_4(SiH_3)_4$	2.34	2.75	2.34
	$In_4(\mu_3\text{-}PbH_3)_4(AlH_3)_4$	1.27	1.67	2.28
	$In_4(\mu_3\text{-}SnH_3)_4(AlH_3)_4$	1.03	1.77	2.09
	$In_4(\mu_3\text{-}GeH_3)_4(AlH_3)_4$	1.08	1.88	2.03
	$In_4(\mu_3\text{-}SiH_3)_4(AlH_3)_4$	0.96	1.87	1.81

[a] Type 0–1 represents that M processes zero and one valence electron to interact with LA and LB, respectively. [b] $Ba_4(\mu_3\text{-}PbH_3)_4(SiH_3)_4$ is instable with an imaginary frequency.

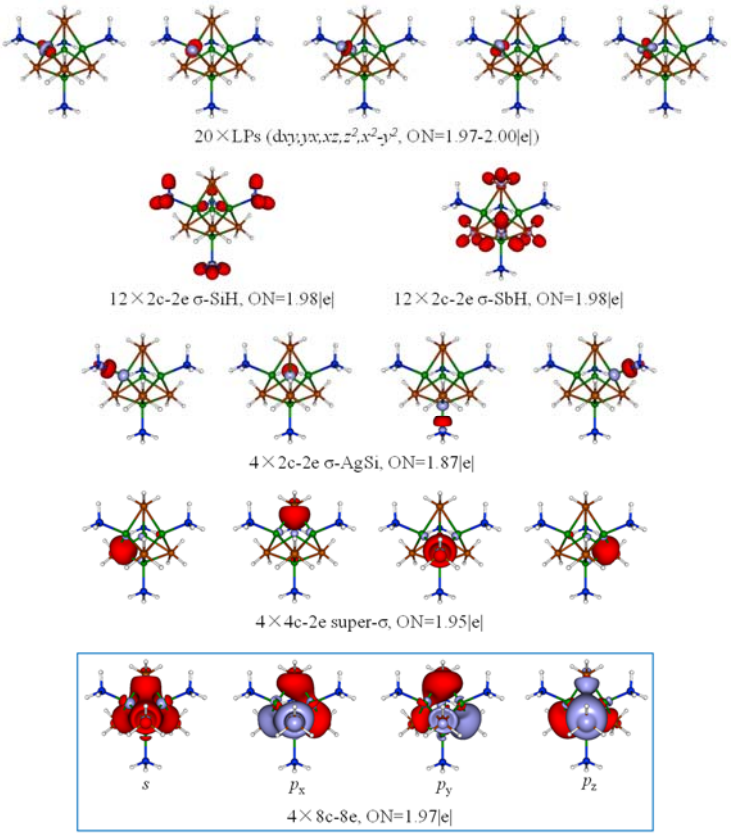

Fig. 4 Bonding pattern for T_d [Ag$_4$(μ_3-SbH$_3$)$_4$(SiH$_3$)$_4$] cluster as revealed from the AdNDP analysis.

Occupation numbers (ONs) are shown.

no longer enough π-back-donation to keep Ag$_4$ core, and the $E_{b\text{-}v}$ of [Ag$_4$(μ_3-SbH$_3$)$_4$(BH$_3$)$_4$], being even less than half of that of [Pd$_4$(μ_3-SbH$_3$)$_4$(SbH$_3$)$_4$], so too the other analogues.

The chemical bonding analyses of the series of analogues are also given by AdNDP method. One example is [Ag$_4$(μ_3-SbH$_3$)$_4$(SiH$_3$)$_4$], which has the same valence electrons with [Pd$_4$(μ_3-SbH$_3$)$_4$(SbH$_3$)$_4$] (Ag $4d^{10}5s^1$ *versus* Pd $4d^{10}$, Si $3s^23p^2$ *versus* Sb $5s^25p^3$). The [Ag$_4$(μ_3-SbH$_3$)$_4$(SiH$_3$)$_4$] (Fig. 4) features a similar bonding pattern of [Pd$_4$(μ_3-SbH$_3$)$_4$(SbH$_3$)$_4$], with twenty lone pairs (*dxy*, *yz*, *xz*, x^2-y^2, z^2), twelve Si—H σ bonds, twelve Sb—H σ bonds, four terminal Ag—Si σ bonds and four 4c–2e super σ-bonds or four 8c–2e super *S* and $P_{x,y,z}$ orbitals.

3.4 Closed-shell interaction

Note that the calculated Pd-Pd distance is 0.2792 nm, which turns out to be longer than a single bond (0.2400 nm) [54] but remarkably smaller than the van der Waals radius. The four Pd atoms are in Pd(0) configuration, the interaction in Pd$_4$ tetrahedron that is similar to aurophilicity in Au-Au clusters [55–59]. It is also found that there are large difference of stability between transition metal clusters and non-transition metal clusters.

For all of the reasons mentioned above, to verify the existence of closed-shell interaction in this Pd-Pd cluster, we futher design two model clusters, T_d Ag$_4$Cl$_4$ and T_d K$_4$Cl$_4$. The structures of two model clusters are remarkably similar with respect to Pd$_4$(SbH$_3$)$_4$ motifs in Pd$_4$(μ_3-SbH$_3$)$_4$(SbH$_3$)$_4$, despite

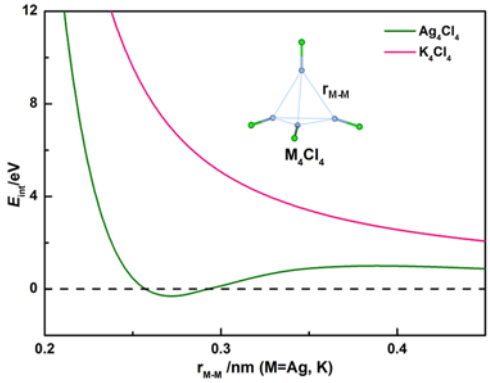

Fig. 5 BSSE-corrected dissociation energy curves of M–M (M = Ag, K) interaction.

the imaginary frequencies they have. Curves for the M–M (M = Ag, K) interaction energy (E_{int} = 4E[MCl] - E[M$_4$Cl$_4$]) of two model clusters as the M-M distance are illustrated in Fig. 5. There is one trough of E_{int} curve in Ag$_4$Cl$_4$ cluster, where the E_{int} values are negative, indicating the attractive interaction between Ag atoms, however, K$_4$Cl$_4$ is not. This is because the former has d^{10} valence electrons but the latter does not. It is necessary to point out that $d^{10}\cdots d^{10}$ interaction can stabilize the pd$_4$ tetrahedron structure.

4 Concliusions

In summary, we present the structure and chemical bonding

of T_d [$Pd_4(\mu_3\text{-}SbH_3)_4(SbH_3)_4$] and the series of analogues by the computational study. Each Pd atom in Pd_4(0) tetrahedron is coordinated to one terminal Sb atom and three bridging Sb atoms with sp^3 hybridization, fulfilling with 4*d*, 5*s* and 5*p* orbitals, rendering 18-electrons principle. In terms of [$Pd_4(\mu_3\text{-}SbH_3)_4$] motifs, it can be not only viewed as a network of four 4c–2e superatoms capping on Pd_4 core or a 8e shell with four 4c–2e super σ-bonds based on SAN and SVB model, but also as a 8e-superatom with $1S^21P^6$ jellium closed-shell configuration. At the same time, the $d^{10}\cdots d^{10}$ interaction plays a critical role in stabilizing the Pd_4 tetrahedron structure. The [$Pd_4(\mu_3\text{-}SbH_3)_4(SbH_3)_4$] is demonstrated to be stable with a filled electronic shell, a large HOMO-LUMO gap and negative NICS value, and the NICSzz-scan suggests that the aromaticity of [$Pd_4(\mu_3\text{-}SbH_3)_4(SbH_3)_4$] can be derived from $Pd_4(\mu_3\text{-}SbH_3)_4$. Moreover, the calculations of energies and bonging analysis of AdNDP reveal that these designed Ag and Cd analogues are also stable structures though they are not better than [$Pd_4(\mu_3\text{-}SbH_3)_4(SbH_3)_4$], but still being significant in designing and synthesizing such metal clusters.

Acknowledgment: The calculations were carried out at the High-Performance Computing Center of Anhui University.

References

(1) Walter, M.; Akola, J.; Lopez-Acevedo, O.; Jadzinsky, P. D.; Calero, G.; Ackerson, C. J.; Whetten, R. L.; Gronbeck, H.; Hakkinen, H. *Proc. Natl. Acad. Sci. USA* **2008,** *105*, 9157. doi: 10.1073/pnas.0801001105

(2) Reber, A. C.; Khanna, S. N. *Acc. Chem. Res.* **2017,** *50*, 255. doi: 10.1021/acs.accounts.6b00464

(3) Dhayal, R. S.; Liao, J. H.; Liu, Y. C.; Chiang, M. H.; Kahlal, S.; Saillard, J. Y.; Liu, C. W. *Angew. Chem. Int. Ed.* **2015,** *54*, 3702. doi: 10.1002/anie.201410332

(4) Malola, S.; Lehtovaara, L.; Knoppe, S.; Hu, K. J.; Palmer, R. E.; Burgi, T.; Hakkinen, H. *J. Am. Chem. Soc.* **2012,** *134*, 19560. doi: 10.1021/ja309619n

(5) Chauhan, V.; Reber, A. C.; Khanna, S. N. *J. Am. Chem. Soc.* **2017,** *139*, 1871. doi: 10.1021/jacs.6b09416

(6) Wan, X. K.; Lin, Z. W.; Wang, Q. M. *J. Am. Chem. Soc.* **2012,** *134*, 14750. doi: 10.1021/ja307256b

(7) Qian, H. F.; Eckenhoff, W. T.; Zhu, Y.; Pintaue, T.; Jin, R. C. *J. Am. Chem. Soc.* **2010,** *132*, 8280. doi: 10.1021/ja103592z

(8) Yuan, S. F.; Li, P.; Tang, Q.; Wan, X. K.; Nan, Z. A.; Jiang, D. E.; Wang, Q. M. *Nanoscale* **2017,** *9*, 11405. doi: 10.1039/c7nr02687k

(9) Geitner, F. S.; Dums, J. V.; Fassler, T. F. *J. Am. Chem. Soc.* **2017,** *139*, 11933. doi: 10.1021/jacs.7b05834

(10) Zhu, M. Z.; Lanni, E.; Garg, N.; Bier, M. E.; Jin, R. C. *J. Am. Chem. Soc.* **2008,** *130*, 1138. doi: 10.1021/ja0782448

(11) Xu, W. W.; Zhu, B.; Zeng, X. C.; Gao, Y. *Nat. Commun.* **2016,** *7*, 13574. doi: 10.1038/ncomms13574

(12) Zhu, M.; Li, M. B.; Yao, C. H.; Xia, N.; Zhao, Y.; Yan, N.; Liao, L. W.; Wu, Z. K. *Acta Phys. -Chim. Sin.* **2018,** (in press) [祝敏, 李漫波, 姚传好, 夏楠, 赵燕, 闫楠, 廖玲文, 伍志鲲. 物理化学学报, **2018,** (in press)] doi: 10.3866/PKU.WHXB201710091

(13) Wu, X. W.; Yi, G. *Acta Phys. -Chim. Sin.* **2018,** (in press) [许文武, 高嶷. 物理化学学报, **2018,** (in press)] doi: 10.3866/ PKU.WHXB201711061

(14) Tominaga, C.; Hikosou, D.; Osaka, I.; Kawasak, H. *Acta Phys. -Chim. Sin.* **2018,** (in press) [Tominaga, C.; Hikosou, D.; Osaka, I.; Kawasak, H. 物理化学学报, **2018,** (in press)] doi: 10.3866/PKU.WHXB201710271

(15) Roach, P. J.; Reber, A. C.; Woodward, W. H.; Khanna, S. N.; Castleman, A. W., Jr. *Proc. Natl. Acad. Sci. USA* **2007,** *104*, 14565. doi: 10.1073/pnas.0706613104

(16) Knight, W. D.; Clemenger, K.; de Heer, W. A.; Saunders, W. A.; Chou, M. Y.; Cohen, M. L. *Phys. Rev. Lett.* **1984,** *52*, 2141. doi: 10.1103/PhysRevLett.52.2141

(17) Clemenger, K. *Phys. Rev. B* **1985,** *32*, 1359. doi: 10.1103/PhysRevB.32.1359

(18) de Heer, W. A. *Rev. Mod. Phys.* **1993,** *65*, 611. doi: 10.1103/RevModPhys.65.611

(19) Khanna, S. N.; Jena, P. *Phys. Rev. B* **1995,** *51*, 13705. doi: 10.1103/PhysRevB.51.13705

(20) Bergeron, D. E.; Castleman, A. W.; Morisato, T.; Khanna, S. N. *Science* **2004,** *304*, 84. doi: 10.1126/science.1093902

(21) Bergeron, D. E.; Roach, P. J.; Castleman, A. W.; Jones, N.; Khanna, S. N. *Science* **2005,** *307*, 231. doi: 10.1126/science.1105820

(22) Castleman, A. W.; Khanna, S. N. *J. Phys. Chem. C* **2009,** *113*, 2664. doi: 10.1021/jp806850h

(23) Luo, Z.; Castleman, A. W. *Acc. Chem. Res.* **2014,** *47*, 2931. doi: 10.1021/ar5001583

(24) Cheng, L. J.; Yuan, Y.; Zheng, X. Z.; Yang, J. L. *Angew. Chem. Int. Ed.* **2013,** *52*, 9035. doi: 10.1002/anie.201302926

(25) Gutrath, B. S.; Oppel, I. M.; Presly, O.; Beljakov, I.; Meded, V.; Wenzel, W.; Simon, U. *Angew. Chem. Int. Ed.* **2013,** *52*, 3529. doi: 10.1002/anie.201208681

(26) Koyasu, K.; Tsukuda, T. *Phys. Chem. Chem. Phys.* **2014,** *16*, 21717. doi: 10.1039/c4cp03199g

(27) Yan, L. J.; Cheng, L. J.; Yang, J. L. *Chin. J. Chem. Phys.* **2015,** *28*, 476. doi: 10.1063/1674-0068/28/cjcp1505105

(28) Cheng, L.; Ren, C.; Zhang, X.; Yang, J. *Nanoscale* **2013,** *5*, 1475. doi: 10.1039/c2nr32888g

(29) Liu, L. R.; Li, P.; Yuan, L. F.; Cheng, L. J.; Yang, J. L. *Nanoscale* **2016,** *8*, 12787. doi: 10.1039/c6nr01998f

(30) Cheng, L. J.; Zhang, X. Z.; Jin, B. K.; Yang, J. L. *Nanoscale* **2014,** *6*, 12440. doi: 10.1039/c4nr03550j

(31) Wang, H. Y.; Cheng, L. J. *Nanoscale* **2017,** *9*, 13209. doi: 10.1039/c7nr03114a

(32) Trebbe, R.; Goddard, R.; Rufinska, A.; Seevogel, K.; Porschke, K. R. *Organometallics* **1999,** *18*, 2466. doi: 10.1021/om990239s

(33) Dedieu, A. *Chem. Rev.* **2000,** *100*, 543. doi: 10.1021/cr980407a

(34) Moc, J.; Musaev, D. G.; Morokuma, K. *J. Phys. Chem. A* **2000,** *104*, 11606. doi: 10.1021/jp0022104

(35) Puddephatt, R. J. *J. Org. Chem.* **2017,** *849*, 268. doi: 10.1016/j.jorganchem.2017.01.030

(36) Tang, S.; Eisenstein, O.; Nakao, Y.; Sakaki, S. *Organometallics* **2017,** *36*, 2761. doi: 10.1021/acs.organomet.7b00256

(37) Kalita, B.; Deka, R. C. *J. Am. Chem. Soc.* **2009,** *131*, 13252. doi: 10.1021/ja904119b

(38) Nava, P.; Sierka, M.; Ahlrichs, R. *Phys. Chem. Chem. Phys.* **2003,** *5*, 3372. doi: 10.1039/b303347c

(39) Benjamin, S. L.; Krämer, T.; Levason, W.; Light, M. E.; Macgregor, S. A.; Reid, G. *J. Am. Chem. Soc.* **2016,** *138*, 6964. doi: 10.1021/jacs.6b04060

(40) Zubarev, D. Y.; Boldyrev, A. I. *Phys. Chem. Chem. Phys.* **2008,** *10*, 5207. doi: 10.1039/B804083D

(41) Frisch, M.; Trucks, G.; Schlegel, H. B.; Scuseria, G.; Robb, M.; Cheeseman, J.; Scalmani, G.; Barone, V.; Mennucci, B.; Petersson, G.; *et al. Gaussian 09*, Revision B. 01; Gaussian Inc., Wallingford, CT, 2010.

(42) Varetto, U. Molekel 5.4.0.8, Swiss National Supercomputing Centre, Manno, Switzerland, 2009.

(43) Boldyrev, A. I.; Wang, L. S. *Phys. Chem. Chem. Phys.* **2016,** *18*, 11589. doi: 10.1039/c5cp07465g

(44) Sergeeva, A. P.; Popov, I. A.; Piazza, Z. A.; Li, W. L.; Romanescu, C.; Wang, L. S.; Boldyrev, A. I. *Acc. Chem. Res.* **2014,** *47*, 1349. doi: 10.1021/ar400310g

(45) Popov, I. A.; Jian, T.; Lopez, G. V.; Boldyrev, A. I.; Wang, L. S. *Nat. Commun.* **2015,** *6*, 8654. doi: 10.1038/ncomms9654

(46) Li, W. L.; Jian, T.; Chen, X.; Chen, T. T.; Lopez, G. V.; Li, J.; Wang, L. S. *Angew.Chem.* **2016,** *128*, 7484. doi: 10.1002/ange.201601548

(47) Xu, C.; Cheng, L. J.; Yang, J. L. *J. Chem. Phys.* **2014,** *141*, 124301. doi: 10.1063/1.4895727

(48) Li, L. F.; Xu, C.; Jin, B. K.; Cheng, L. J. *Dalton Trans.* **2014,** *43*, 11739. doi: 10.1039/c4dt01106f

(49) Yuan, Y.; Cheng, L. J. *J. Chem. Phys.* **2013,** *138*, 024301. doi: 10.1063/1.4773281

(50) Li, L. F.; Xu, C.; Jin, B. K.; Cheng, L. J. *J. Chem. Phys.* **2013,** *139*, 174310. doi: 10.1063/1.4827517

(51) Li, L. F.; Xu, C.; Cheng, L. J. *Comput. Theor. Chem.* **2013,** *1021*, 144. doi: 10.1016/j.comptc.2013.07.001

(52) Yuan, Y.; Cheng, L. J. *J. Chem. Phys.* **2012,** *137*, 044308. doi: 10.1063/1.4738957

(53) Cheng, L. J. *J. Chem. Phys.* **2012,** *136*, 104301. doi: 10.1063/1.3692183

(54) Pyykkö, P. *J. Phys. Chem. A* **2015,** *119*, 2326. doi: 10.1021/jp5065819

(55) Cui, G. L.; Cao, X. Y.; Fang, W. H.; Dolg, M.; Thiel, W. *Angew. Chem. Int. Ed.* **2013,** *52*, 10281. doi: 10.1002/anie.201305487

(56) Pyykkö, P. *Angew. Chem. Int. Ed.* **2004,** *43*, 4412. doi: 10.1002/anie.200300624

(57) Schmidbaur, H.; Schier, A. *Angew. Chem. Int. Ed.* **2015,** *54*, 746. doi: 10.1002/anie.201405936

(58) Pyykkö, P.; Mendizabal, F. *Inorg. Chem.* **1998,** *37*, 3018. doi: 10.1021/ic980121o

(59) Harwell, D. E.; Mortimer, M. D.; Knobler, C. B.; Anet, F. A. L.; Hawthorne, M. F. *J. Am. Chem. Soc.* **1996,** *118*, 2679. doi: 10.1021/ja953976y